Science of the Total Environment 633 (2018) 608–617

Contents lists available at ScienceDirect

Science of the Total Environment

journal homepage: www.elsevier.com/locate/scitotenv

De-coupling interannual variations of vertical dust extinction over the Taklimakan Desert during 2007–2016 using CALIOP

Yang Nan [a], Yuxuan Wang [a,b,*]

[a] Ministry of Education Key Laboratory for Earth System Modeling, Department of Earth System Science, Tsinghua University, Beijing 100084, China
[b] Department of Earth & Atmospheric Sciences, University of Houston, Houston, TX 77004, United States

HIGHLIGHTS

- Dust extinction at 4–6 km over TD shows a different interannual variation from that at 1–4 km in springtime.
- The de-coupled variability of dust extinction across 4 km over TD exists only in spring due to the unique topography.
- High dust levels below 4 km over TD are necessary but not sufficient conditions for eastward dust transport.
- Dust extinction above 4 km over TD is more related to dust transport at high altitudes over downwind regions.

GRAPHICAL ABSTRACT

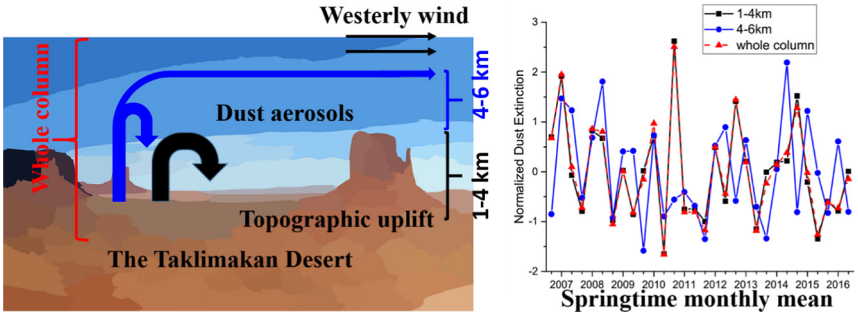

ARTICLE INFO

Article history:
Received 18 January 2018
Received in revised form 7 March 2018
Accepted 11 March 2018
Available online xxxx

Editor: Jianmin Chen

Keywords:
CALIOP
The Taklimakan Desert
Vertical dust extinction
De-coupled interannual variability

ABSTRACT

During the springtime, mineral dust from the Taklimakan Desert (TD) is lifted up to high altitudes and transported long distances by the westerlies. The vertical distributions of Taklimakan dust are important for both long-range transport and climate effects. In this study, we use CALIOP Level 3 dust extinction to describe interannual variation of dust extinction in TD aggregated at each 1 km interval (1–2 km, 2–3 km, 3–4 km, 4–5 km and 5–6 km) above mean sea level during springtime from 2007 to 2016. 87% of dust extinction over TD is concentrated at 1–4 km taking a major composition of dust aerosol optical depth (AOD) and only 8.1% dust AOD is at 4–6 km. Interannual variation of seasonal and monthly dust extinction at 1–4 km is almost as same as dust AOD ($R > 0.99$) but different from that at 4–6 km (R are around 0.42). Our analysis provides observational evidence from CALIOP that vertical dust extinction over TD has distinctively different variability below and above 4 km altitude and this threshold divides dust transport in TD into two systems. Taklimakan dust aerosols are more related to dust transport at high altitudes (4–10 km) than low altitudes (0–4 km) over downwind regions. High dust extinction below 4 km over TD is necessary but not sufficient conditions to ensure dust transport easterly, while high dust extinction levels at 4–6 km over TD are both necessary and sufficient conditions; such contrast leads to the de-coupled interannual variability seen by CALIOP.

Abbreviations: TD, The Taklimakan Desert; GD, The Gobi Desert; TR, A Transported Region.

* Corresponding author at: Department of Earth & Atmospheric Sciences, University of Houston, Houston, TX 77004, United States.
E-mail address: ywang246@central.uh.edu (Y. Wang).

https://doi.org/10.1016/j.scitotenv.2018.03.125
0048-9697/

1. Introduction

Airborne aerosols are an important component of the Earth's atmosphere. They can cause air pollution posing health hazards for humans and affect the radiative budget and hydrological balances of the atmosphere. Globally the largest source of aerosols to the atmosphere is mineral dust generated from the erosion of soil resulting from natural causes as well as significant contributions from human activities. The Sahara Desert in North Africa is the largest source of mineral dust with annual emissions estimated of about 800 Tg. In East Asia, the Taklimakan Desert (TD) and the Gobi Desert (GD) are the two largest dust sources producing about 200 Tg of emissions annually (Tanaka and Chiba, 2006). Seasonally, dust storms over East Asia occur primarily in spring. TD is located in Xinjiang Uyghur Autonomous Region in northwest China, bounded by the Kunlun Mountains to the south, the Pamir Mountains and Tian Shan to the west and north. GD is located to the east of TD. In TD, the prevailing wind direction and hence the direction of sand dunes motion (Sun et al., 2001) are easterly and northeasterly almost all year long. Thus, due to the unique topography, Taklimakan dust lower than 5 km may not be easily transported out of this dessert (Ge et al., 2014), but it can be entrained to above 5 km up to 10 km and transported horizontally over long distances by the westerlies during dust storms (Yumimoto et al., 2009).

The altitudes of Asian dust loading in the atmosphere are important for both long-range transport and climate effects. Case studies show that Taklimakan dust can reach the upper troposphere 4 to 10 km above sea level (MSL) by strong convective updrafts, and then be transported more than one full circuit around the globe in about 13 days (Eguchi et al., 2009; Grousset et al., 2003; Uno et al., 2009; Yumimoto et al., 2009). All the altitudes reported hereafter are above mean sea level (MSL). Eguchi et al. (2009) found a two-layered dust vertical distribution over northeastern Pacific and North America in May 2007: the upper dust cloud (4–10 km) was above the major clouds layer mainly originated from a dust storm of the Taklimakan Desert and probably was unmixed with Asian air pollutants; the lower dust layer (0–4 km) was largely generated from a dust storm of the Gobi Desert and well mixed with anthropogenic aerosols. In addition, the radiative effects of Asian dust are significantly determined by the vertical distributions (Huang et al., 2014). The net dust aerosol climate effects (direct, indirect, and semidirect effects) are still highly uncertain. The model simulations of aerosol vertical distributions differ up to one order of magnitude leading to large uncertainties of climate effects (Textor et al., 2006). In this study, we examine the vertical distributions of dust particles over TD and downwind regions using satellite observations.

The Cloud-Aerosol Lidar with Orthogonal Polarization (CALIOP), carried on The Cloud-Aerosol Lidar and Infrared Pathfinder Satellite Observations (CALIPSO) has been acquiring the first-ever, continuous multiyear global aerosol and cloud profile data since June 2006 (Winker et al., 2010). Based on the active lidars of particulate depolarization ratio at 532 nm with a near zero depolarization ratio for spherical particles, CALIOP can effectively distinguish non-spherical aerosol (e.g. dust, volcanic ash) from spherical aerosols (e.g. industrial pollution, biomass burning smoke, and marine aerosol) (Winker et al., 2009). CALIOP aerosol profiles provide quantitative characterization of elevated aerosol layers in major transport pathways. Yu et al. (2012) estimated based on CALIOP and the Moderate Resolution Imaging Spectroradiometer (MODIS) aerosol products that on an annual bias, 140 Tg of dust is exported from East Asia, of which 56 Tg reaches North America. The zonal bands of 30°–40° N and 40°–50° N are major transport routes of Asian dust with 10–20 Tg of annual dust flux respectively, and the band of 50°–60° N is a minor route with about 5 Tg of annual eastward dust flux. The annual trans-Pacific dust transport (120–130 Tg of dust) occurs mainly above the boundary layer with 90–100 Tg of dust above 5 km. The two-layer dust structure over East China and the Pacific Ocean results from the combination of the two Asian dust sources (i.e. TD and GD) with the Taklimakan dust particularly at high altitudes (Eguchi et al., 2009; Huang et al., 2008; Uno et al., 2008).

While the vertical cross-section of the CALIOP dust extinction has been widely used to investigate vertical structures of dust storm episodes individually, few studies have provided longer-term observational evidence for the relationship between the vertical extent of Taklimakan dust and its transport impacts. Liu et al. (2008) provided a height resolved global view of dust aerosols from the first year CALIPSO lidar measurements, which just describes seasonal dust layer vertical extent over East Asia. Yu et al. (2010) discussed aerosol vertical distribution over East Asia using one-year CALIOP data. Yu et al. (2012) estimated vertical dust outflow from Asia using four-year CALIOP data and six-year MODIS data. The CALIOP dataset covering June 2006 to present provides a decade-long record of aerosol profiles, which allow us to investigate the interannual variations of vertical distribution of Taklimakan dust and aerosols over downwind regions. In this study, we use the CALIOP Level 3 Aerosol Profile products in springtime during the period from 2007 to 2016. Section 2 briefly describes the CALIOP Level 3 aerosol retrievals. Section 3 presents the de-coupling of interannual variations of dust extinction profiles and dust aerosol optical depth (AOD) over TD derived from CALIOP, which is found to exist only in spring. In Section 4, we discuss mechanisms and transport impacts. Lastly, concluding remarks are given in Section 5.

2. CALIOP data

CALIPSO was launched in April 2006 and is a part of the A-train constellation of satellites. The A-train satellites give a 16-day cycle, crossing the equator northbound at about 1330 local time. As the primary instrument carried on the CALIPSO satellite, CALIOP is the first polarization lidar to provide global, 3-D measurements of atmospheric aerosols (Winker et al., 2009). CALIOP acquires lidar backscatter profiles at 532 nm and 1064 nm, containing parallel and perpendicular polarized returns at 532 nm. The vertical sample resolution is 30 m up to 8.2 km and 60 m between 8.2 km and 20.2 km. A cloud-aerosol discrimination (CAD) algorithm is used to distinguish cloud and aerosol in the retrieval (Liu et al., 2009). At each aerosol layer, aerosols are classified into 6 specific types: dust, smoke, clean continental, polluted continental, clean marine, and polluted dust. Each aerosol type is assumed to have a consistent lidar ratio, S_a (the ratio of aerosol 180-backscatter to extinction), which is used to retrieve aerosol extinction by type (Omar et al., 2009; Winker et al., 2009).

CALIOP Level 2 products contain height-resolved geophysical parameters such as aerosol backscatter, extinction, depolarization and aerosol typing classifications along the CALIPSO tracks. The Level 3 (L3) products are aggregated from the Level 2 data and gridded at a global resolution of 2° (latitude) × 5° (longitude). In this study, we used the CALIOP Version 3, Level 3, monthly-mean gridded aerosol extinction data at 532 nm covering the springtime (i.e. March, April, and May; MAM) periods from 2007 to 2016. The vertical resolution of the gridded Level 3 products is 60 m from the surface up to 12 km. Only nighttime data were used because the quality of CALIOP daytime retrievals is degraded by the interference of sunlight (Winker et al., 2009; Yu et al., 2015). The comparison between daytime and nighttime data is shown in the supplementary material (Fig. S1 and Table S1). CALIOP L3 monthly mean extinction profiles are classified into four sky conditions: all-sky, cloud-free (no cloud), cloudy-sky-transparent (thin cloud), and cloudy-sky-opaque (thick cloud). Data under the all-sky conditions is the weighted mean of all the other sky conditions. In the rest of this section, we define the horizontal and vertical study coverage of TD by CALIOP data and examine whether CALIOP AOD has a good agreement with MODIS AOD on interannual variation over TD.

Fig. 1 shows the spatial distribution of springtime nighttime CALIOP-retrieved dust AOD (Fig. 1a) and the ratio of dust AOD to AOD (Fig. 1b) over East Asia during 2007–2016. TD is defined geographically as the

region between 35°–43° N and 75°–90° E (black rectangle in Fig. 1). Dust AOD has a maximum regional-mean of 0.47 over TD and then decreases eastward to lower than 0.3. Dust AOD accounts for 97.4% of AOD over TD, indicating most of the aerosols are mineral dust. By comparison, dust AOD contributes to 79% of AOD over GD (39°–45° N and 95°–110° E), the second largest dust source in China. Once lifted above the boundary layer, dust emitted from TD and GD can be transported over long distances by the mid-latitude westerlies. For other regions over East China, the ratio of dust AOD to AOD is typically <50%. The main transport routes of Asian dust are within 30°–50° N showing both high levels of dust AOD and the ratio of dust AOD to AOD, consistent with previous studies (Eguchi et al., 2009; Yu et al., 2012).

Fig. 2 compares the mean dust extinction profiles (Fig. 2a) and the number of accepted dust samples (Fig. 2b) over TD during MAM of 2007–2016 under the four sky conditions described above. Accepted dust samples report dust aerosol samples in each 3-D grid cell of CALIOP L3 data that were detected and passed all quality assurance filtering criteria (https://www-calipso.larc.nasa.gov/resources/calipso_users_guide/data_summaries/l3/index.php#samplesaerosoldetectedacceptedduspolluteddustsmoke). The extinction profile under the all-sky conditions is the weighted mean extinction of the other three sky conditions. Under the all-sky, cloud-free, and cloudy-sky-transparent conditions, dust extinction increases rapidly from 0.01 km^{-1} at 0.8 km to above 0.1 km^{-1} between 1 km and 3.3 km with peaks at around 1.5 km. The extinction decreases gradually to 0.01 km^{-1} from 3.3 km to 6 km and maintains an extremely low value above 6 km. Under the cloudy-sky-opaque conditions, dust extinction has distinct values only between 3.3 km and 4.3 km with a maximum of about 0.01 km^{-1}. Dust extinction below 3.3 km may be underestimated in this case due to screening out aerosols under the thick clouds. However, the number of accepted dust samples under the cloudy-sky-opaque conditions is far less than that of the other sky conditions, therefore minimizing the influence of such bias on dust extinction averaged under the all-sky conditions. All-sky dust extinction accounts for almost all of the AOD between 1 km and 6 km. Therefore, all the CALIOP data shown hereafter are under the all-sky conditions (L3 nighttime products at 532 nm) during the spring months (MAM) of 2007–2016, unless stated otherwise.

AOD retrievals from MODIS have been widely used to investigate aerosol optical properties because of their extensive coverage and high quality. Here we used the L3 550 nm AOD from MODIS on Aqua retrieved by the Deep Blue algorithm, which is designed to retrieve aerosols over bright surfaces such as deserts (Hsu et al., 2006; Sayer et al., 2013). Fig. 3 compares the MODIS and CALIOP AOD over TD during MAM of 2007–2016. The springtime mean AOD from CALIOP is consistently lower than the Deep Blue AOD from MODIS-Aqua by about 20%, similar to previous results (Ma et al., 2013; Redemann et al., 2012; Yu et al., 2010). The regional-mean AOD and dust AOD from CALIOP are 19% and 21% lower than the Deep Blue AOD from MODIS-Aqua respectively. Despite this difference, the interannual variations of AOD and dust AOD from CALIOP are consistent with those from MODIS. The temporal correlation coefficients between the two products (i.e. MODIS Deep Blue AOD and CALIOP AOD) are 0.19 for the seasonal mean and 0.62 for the monthly mean. The low coefficient for the seasonal mean is mainly due to the AOD difference of 2016, although month-to-month variations within 2016 are similar between the two products. The correlation coefficients between the two products increase to 0.61 for the seasonal mean and 0.74 for the monthly mean after excluding the 2016 data. Dust extinction from CALIOP, which is the major composition (about 97%) of CALIOP AOD over TD, shows a slightly higher correlation with MODIS Deep Blue AOD on the interannual time scale. The difference between CALIOP and MODIS AOD over TD can be explained in part by the fact that CALIOP AOD is the nighttime data and MODIS Deep Blue AOD is the daytime data and the two instruments retrieve AOD at different wavelengths. In spite of the differences (Kim et al., 2013; Ma et al., 2013; Redemann et al., 2012), CALIOP AOD has a good agreement with MODIS AOD in terms of interannual variation over TD, which is the focus of this study.

3. De-coupled variability of vertical dust extinction over TD

3.1. Springtime

In this section, we examine the interannual variations of dust extinction vertical profiles over TD during MAM of 2007–2016. Despite the fine vertical resolution (60 m) of the CALIOP L3 aerosol extinction products, we integrated dust extinction over each 1 km interval between 1 km and 6 km (i.e. 1–2 km, 2–3 km, 3–4 km, 4–5 km and 5–6 km) to reduce the likely impacts of random errors from sampling on dust aerosol extinction profiles (Fig. 2a). Fig. 4 shows the breakdown of mean dust AOD over TD by altitude. Dust extinction below 4 km accounts for about 87% of the total dust AOD, and the fraction is 6.54%, 1.55%, and 0.66% at 4–5 km, 5–6 km, and above 6 km, respectively.

Dust extinction decreases dramatically with altitude; the mean extinction at each 1 km interval is 0.186 (1–2 km), 0.143 (2–3 km), 0.082 (3–4 km), 0.031 (4–5 km), and 0.007 (5–6 km). Fig. 5a shows the normalized time series of dust extinction by altitude. Normalized Dust Extinction (NDE) was calculated as follows:

$$NDE = (DE - \mu)/\sigma$$

where DE, μ and σ are dust extinction, ten-year springtime mean dust extinction and standard deviation of ten-year springtime dust

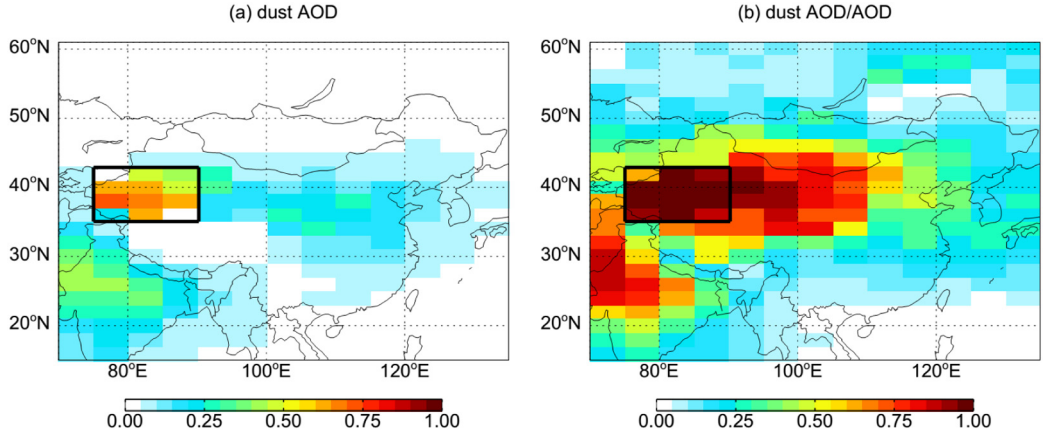

Fig. 1. Springtime (March, April, and May; MAM) nighttime mean CALIOP dust AOD (a) and the ratio of dust AOD to AOD (b) during 2007–2016 under the all-sky conditions. The black rectangle shows the study region of the Taklimakan Desert (TD, 75°–90° E, 35°–43° N).

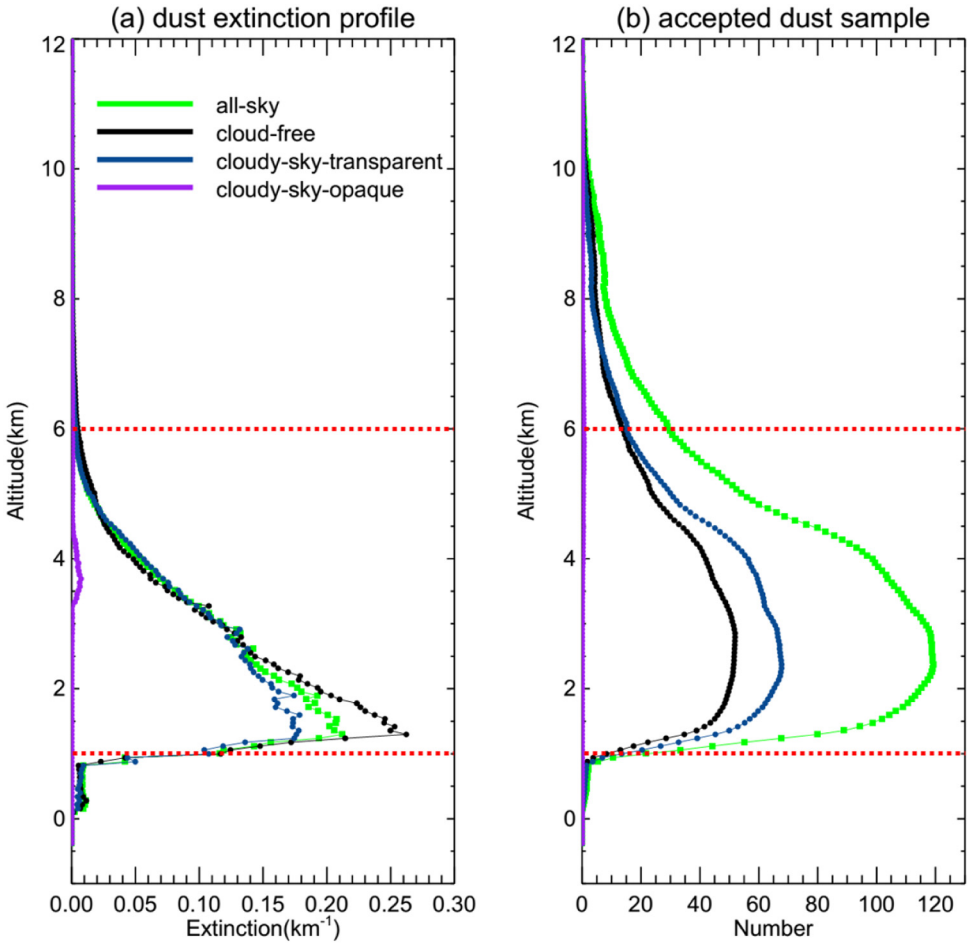

Fig. 2. Mean 532 nm dust extinction profiles (a) and the numbers of accepted dust sample (b) over TD. Data shown are averages of MAM of 2007–2016. Green, black, blue and purple solid lines show dust extinction profiles under the all-sky, cloud-free, cloudy-sky-transparent and cloudy-sky-opaque conditions respectively; the red dotted lines show the vertical study boundaries (1–6 km) of TD. (For interpretation of the references to colour in this figure legend, the reader is referred to the web version of this article.)

extinction over TD during 2007–2016 on seasonal or monthly scales, respectively.

Dust extinction at 1–2 km, 2–3 km and 3–4 km show very similar interannual variations with each other and with the whole column dust AOD, but the variations at 4–5 km and 5–6 km are very different from those below 4 km and the whole column dust AOD. For example, dust extinction below 4 km has a pronounced peak in 2011 and a minimum in 2009, but dust extinction above 4 km had a minimum in 2011 and the 2009 value was close to the 2007–2016 mean. The mean correlation coefficient of dust extinction at each 1 km bin at 1–4 km and at 4–6 km with dust AOD over TD is 0.85 and 0.45 respectively. The largest change in correlation coefficient occurs at 4 km (Table 1).

For simplicity, we further integrated dust extinction over two altitude intervals: 1–4 km and 4–6 km. Fig. 5b shows the normalized time series of these integrated dust extinction. The de-coupled interannual variability between 1–4 km and 4–6 km dust extinction as observed by CALIOP is the focus of our analysis in what follows. This phenomenon also shows up in the monthly-mean time series of dust extinction (Fig. 5c), suggesting the difference exists not only on the seasonal scale but also on the monthly scale to some extent. In the

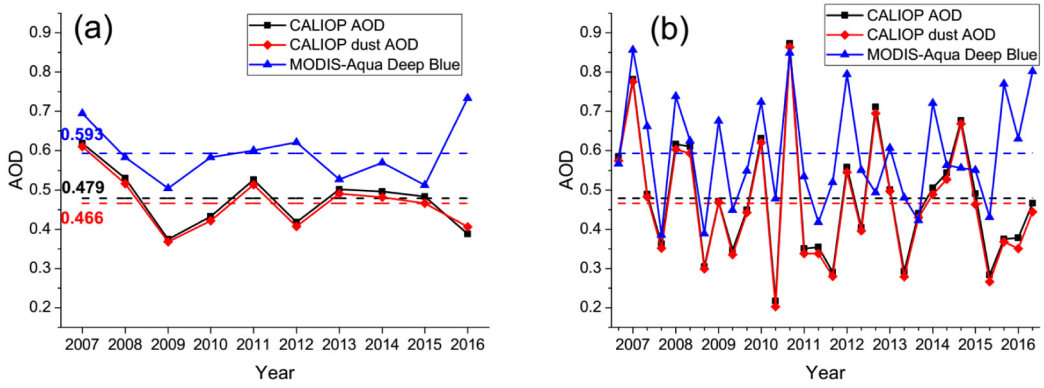

Fig. 3. Time series of seasonal-mean (a) and monthly-mean (b) CALIOP 532 nm AOD (black solid line), dust AOD (red solid line) and MODIS-Aqua Deep Blue 550 nm AOD (blue solid line) over TD during MAM of 2007–2016. The black, red and blue number in Fig. 3a shows multiyear-mean of CALIOP AOD, CALIOP dust AOD, and MODIS Deep Blue AOD. (For interpretation of the references to colour in this figure legend, the reader is referred to the web version of this article.)

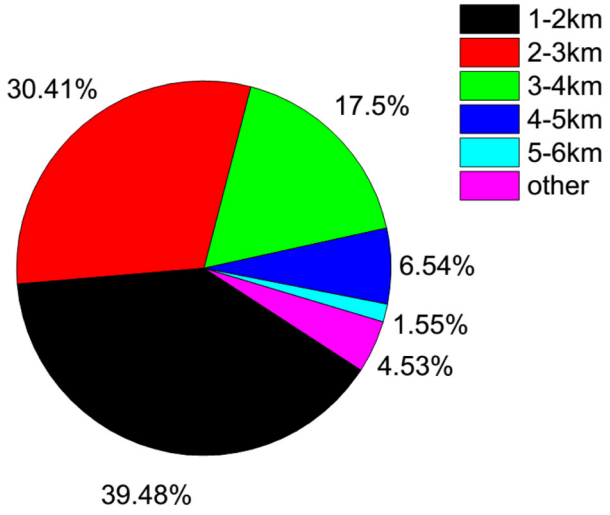

Fig. 4. The breakdown of mean CALIOP dust AOD over TD by altitude during MAM of 2007–2016.

supplementary material (Table S2), we verified that the variations shown in Figs. 5a, 5b and 5c are not caused by sampling biases of CALIOP at different altitudes.

3.2. Other seasons

Since we found the de-coupled variability of dust extinction at 1–4 km and 4–6 km over TD in spring, this section examines if the same phenomenon exists in other seasons. We first compared CALIOP AOD and dust AOD over TD with the MODIS Deep Blue AOD during all the months of 2007–2016 (Fig. S2a), using the same datasets described in Section 2. The multi-year mean AOD from CALIOP (0.328) is higher than the Deep Blue AOD from MODIS-Aqua (0.307) by 6.8%. Dust AOD counts for about 87.8% of the CALIOP AOD, suggesting dust is consistently the major composition over TD in all the seasons. Both AOD and dust AOD have distinct seasonal variations with a peak in spring. When all the months are considered, the interannual variations of AOD and dust AOD from CALIOP show better agreements with MODIS AOD than those in spring only (discussed in Section 2): the temporal correlation coefficients between the two products is 0.82 for AOD and 0.85 for dust AOD. Fig. S2b shows the multi-year mean annual cycle of MODIS-Aqua Deep Blue AOD, CALIOP AOD, and CALIOP dust AOD during 2007–2016. As shown in Table 2, the orders of seasonal AOD and the ratios of dust AOD to AOD are both: MAM > JJA (i.e. June, July, and August) > SON (i.e. September, October, and November) > DJF (i.e. December, January, and February). MODIS Deep Blue AOD is consistently higher than CALIOP AOD in the springtime but lower in other seasons.

Table 1
Correlation coefficients of seasonal and monthly mean CALIOP dust AOD with dust extinction at 1 km bin over TD during spring of 2007–2016.

Altitude(km)	1–2	2–3	3–4	4–5	5–6
R(seasonal)	0.904	0.843	0.791	0.471	0.552
R(monthly)	0.869	0.944	0.702	0.353	0.163
Altitude(km)	1–4			4–6	
R(seasonal)	0.995			0.522	
R(monthly)	0.993			0.319	

The de-coupled variability of dust AOD across 4 km over TD is found to exist only in spring. Dust AOD accounts for 62.9% of AOD over TD in wintertime (i.e. DJF) and only 1.9% of dust AOD are at 4–6 km, both values being much lower than those of the other seasons (Table 2) suggesting much fewer dust particles can be uplifted up to above 4 km in winter. The de-coupling of dust extinction at each 1 km bin with dust AOD happens at around 5 km and 3 km in summer (i.e. JJA) and fall (i.e. SON) respectively (not shown), using the same method in Section 3.1. In addition, dust AOD at 1–4 km in summer and fall is <65% of that in spring, suggesting less and/or weaker dust events in TD.

Thus, the CALIOP L3 data presented above suggests the de-coupling of monthly-mean dust extinction between 1–4 km and 4–6 km over TD only occurs in spring. In this season, the correlation coefficient between dust AOD and dust extinction at each 1 km bin below 4 km is large and significantly decreases above 4 km, suggesting an altitude threshold for Taklimakan dust. In next section, we discuss mechanisms and transport impacts.

4. Discussions

4.1. Mechanisms

Previous AOD studies showed that dust storm events are responsible for high levels of dust extinction and AOD over TD and even the whole East Asia region (Ginoux et al., 2012; Hsu et al., 2006; Huang et al., 2008). AOD reaches high levels during dust episodes. However, these

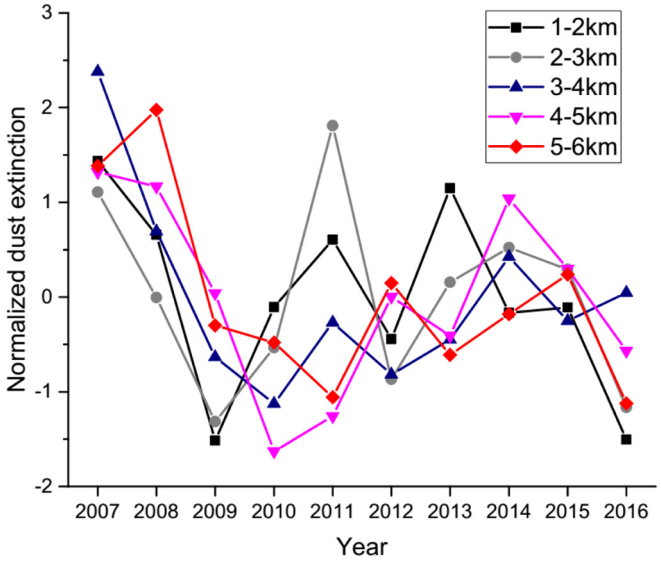

Fig. 5a. Time series of normalized seasonal-mean CALIOP dust extinction (km^{-1}) at each 1 km bin between 1 km and 6 km over TD during MAM of 2007–2015.

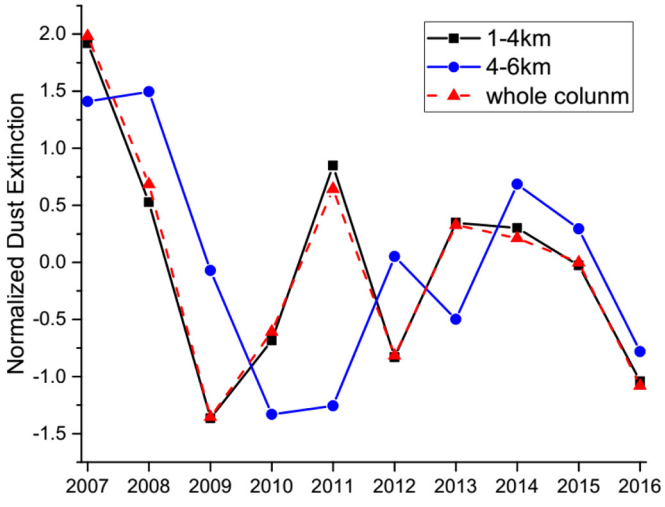

Fig. 5b. Normalized seasonal-mean dust extinction at 1–4 km (black solid line) and 4–6 km (blue solid line) and whole column dust AOD (red dash line) over TD during MAM of 2007–2016. (For interpretation of the references to colour in this figure legend, the reader is referred to the web version of this article.)

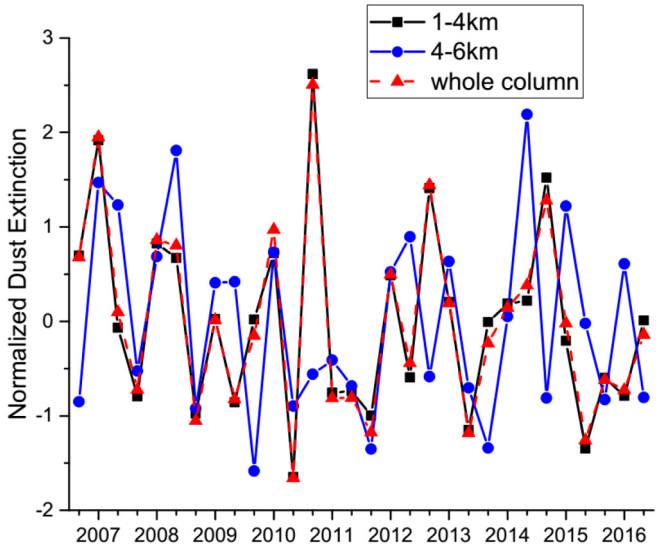

Fig. 5c. Same as Fig. 5b, but for monthly-mean.

studies focused primarily on dust extinction or AOD integrated over the whole column, which may not be applicable to explain the de-coupled variability in dust extinction between 1–4 km and 4–6 km presented above.

The unique topography around TD and the occurrence frequency of dust events in TD lead to a complex mechanism of dust transport. Geographically, TD is surrounded by high mountains (average > 5 km) to the north, west, and south (Fig. 6). The thresholds of altitude around TD are around 4 km shown in Fig. 6d. The prevailing wind directions in TD is easterly and northeasterly almost all year long (Ge et al., 2014; Sun et al., 2001). Thus, dust at elevations below 4 km cannot be easily transported out of this dessert (Huang et al., 2014; Sun et al., 2001). It is only when Taklimakan dust particles are uplifted above 4 km and entrained in the westerlies that they begin to undergo long-range transport. Huang et al. (2008) reported that the majority (91.1%) occurrence frequency of dust events in TD is the weak dust event ("floating dust") with only 1.4% of those is dust storm using surface observations. Dust particles during dust storms are more likely to be lifted up to high altitudes above 4 km, while those during weak dust events cannot. Model simulations of a dust storm in May 2007 supported this mechanism (Eguchi et al., 2009; Uno et al., 2009; Yumimoto et al., 2009). Dust extinction below 4 km and above 4 km results mainly from the most frequently weak dust events and the occasional dust storms, respectively. Chen et al. (2014) estimated that about 50% of dust aerosols are deposited locally over TD because of the unique topography. Only 25% and 23% of Taklimakan dust is transported to other areas over East Asia in spring and summer, respectively (Chen et al., 2017). The CALIOP dust extinction is an indicator of dust distribution, which results from the combination of sources, transport, and other factors affecting dust distribution. We use the occurrence frequency of dust events in TD to explain the mechanisms of the de-coupled interannual variability of dust extinction over TD, suggesting that the satellite data have the potential to be used to investigate the meteorological drivers.

Our analysis above provides observational evidence from CALIOP that vertical dust extinction over TD has distinctively different variability below and above 4 km altitude and this threshold divides dust transport in TD into two systems qualitatively. There is a relatively stable system of closed-loop dust transport under 4 km. Dust aerosols during weak dust events are lifted up, blocked by high mountains, and then deposited locally leading to the same levels of dust source and sink. Dust aerosols during dust storms can be transported easterly above 4 km, leading to lower local deposition of dust than the source. Thus, the de-coupled variability is a manifestation of the two separate vertical systems of dust transport over TD. Since only dust above 4 km can be transported outside of TD, we examine the relationship between dust extinction at 4–6 km over TD and dust transport impacts in the next section.

Table 2
Seasonal-mean information of CALIOP vertical dust AOD distribution over TD during all seasons of 2007–2016.

Season	DJF	MAM	JJA	SON
Dust AOD	0.153	0.466	0.313	0.217
Ratio of dust AOD to AOD (%)	62.9	97.4	91.3	88.7
Dust AOD (1–4 km)	0.138	0.411	0.257	0.195
Ratio of dust AOD (1–4 km) to dust AOD (%)	91.7	88.2	82.3	90.1
Dust AOD (4–6 km)	0.003	0.038	0.047	0.013
Ratio of dust AOD (4–6 km) to dust AOD (%)	1.9	8.2	14.9	6.2

4.2. Transport impacts

Fig. 7 shows two layers of multiyear-mean dust AOD and the ratio of dust AOD to AOD over China: the upper layer (4–10 km) and the lower layer (0–4 km). The splitting of 0–4 km and 4–10 km is chosen somewhat arbitrarily so that we can better explain the transport impacts of the de-coupled variability of dust extinction across 4 km over TD. We extend 4–6 km to 4–10 km for the upper layer because Taklimakan dust can reach the upper troposphere 4–10 km by strong convective updrafts, and then be transported eastwards (Eguchi et al., 2009; Grousset et al., 2003; Uno et al., 2009; Yumimoto et al., 2009). For a better display, dust AOD at the upper layer (4–10 km) is multiplied by 10. Dust AOD at 4–10 km shows a clear west-to-east gradient (Fig. 7a), decreasing gradually along longitude from 0.047 at 90°–95°E to 0.026 at 115°–120°E between 33°N and 43° N (Table S3), which indicates the main transport route of Taklimakan dust at the upper layer. The ratio of dust AOD to AOD at 4–10 km maintains high levels (>50%) to the east of 120° E, consistent with this transport route. Dust AOD at 0–4 km does not show the similar distinct gradient at 4–10 km, and increase along longitude from 0.171 at 90°–95°E to 0.394 at 115°–120°E between 33°N and 43° N (Table S3). The ratio of dust AOD to AOD at 0–4 km sharply decreases to <50% to the east of 110° E and even <25% to the east of 120° E. The reduction of the ratio of dust AOD to AOD at 0–4 km is mainly due to high portion (>50%) of polluted dust (i.e. dust mixed with biomass burning smoke and urban pollution) in Fig. S3, while the upper layer is less likely to mix with polluted dust. Thus, we defined a Transported Region (TR, 90°–110° E, 33°–43° N) based on the west-to-east gradient close to TD.

To examine transport impacts of dust extinction at 4–6 km over TD, we defined two groups of the dust extinction at 4–6 km (Table 3). "High_4–6 km" includes those months with monthly mean dust extinction at 4–6 km exceeding the 80th percentile of the whole monthly-mean over TD, and 'Low_4–6 km' contains those not more than the 20th percentile. Thus, the difference between High_4–6 km and Low_4–6 km can be attributed primarily to the effects of dust extinction at 4–6 km over TD. Fig. 8 shows the spatial distributions of dust AOD at 4–10 km and 0–4 km over East Asia under these two conditions during spring of 2007–2016 The regional-mean statistics for vertical dust AOD differences are summarized in Table 3. Compared to the 'Low_4–6 km' conditions, dust AOD over TD under the 'High_4–6 km' conditions increases 34.3% and 308.8% at 1–4 km and 4–6 km, respectively. This suggests that higher levels of dust under 4 km are necessary for uplifting dust aerosols up to above 4 km over TD. The dust AOD differences over TR are +23.7% at 4–10 km and −29.5% at 0–4 km. In addition, dust AOD differences at 4–10 km over TR show a clear west-to-east gradient, decreasing from +89.2% to −29.7%. Thus, Taklimakan dust aerosols are more related to dust transport at high altitudes (4–10 km) than low altitudes (0–4 km) over the downwind regions.

To distinguish the transport effects of the de-coupled interannual variability, we also defined 'High_1–4 km' and 'Low_1–4 km' in Table

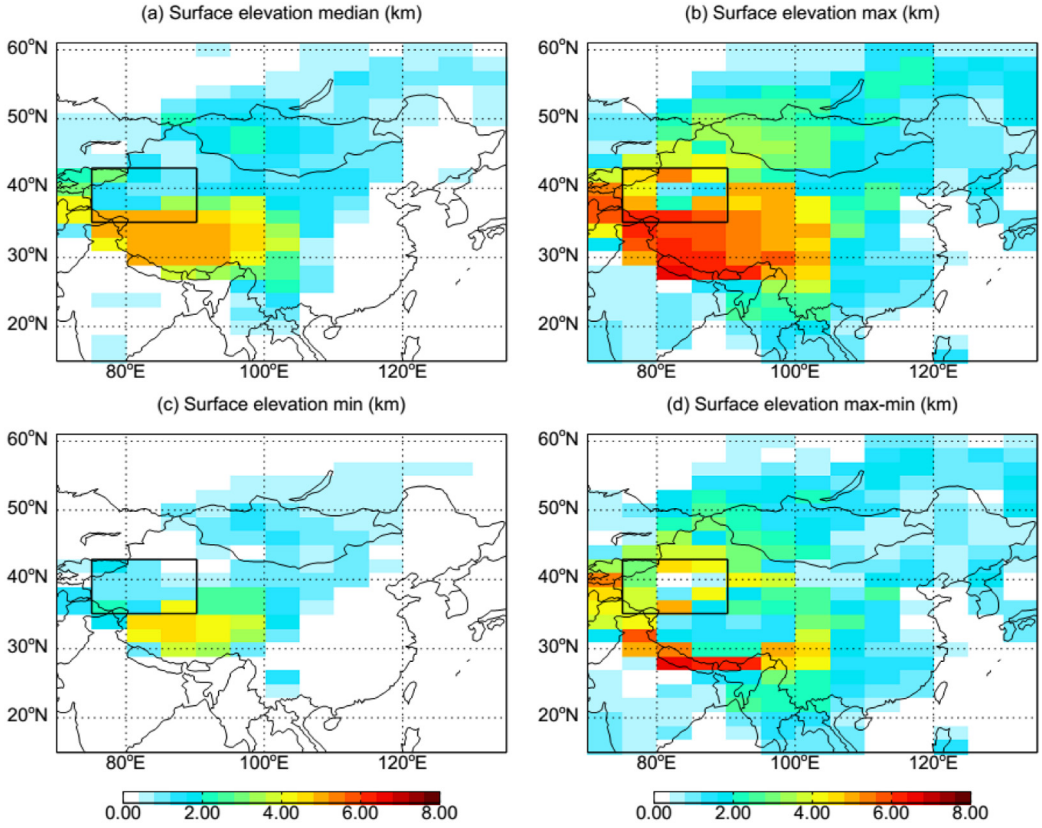

Fig. 6. Surface elevation statics for all columns in grid cell in kilometers above local mean sea level, obtained from CALIOP Version 3, Level 3 data. The black rectangle shows the study region of TD.

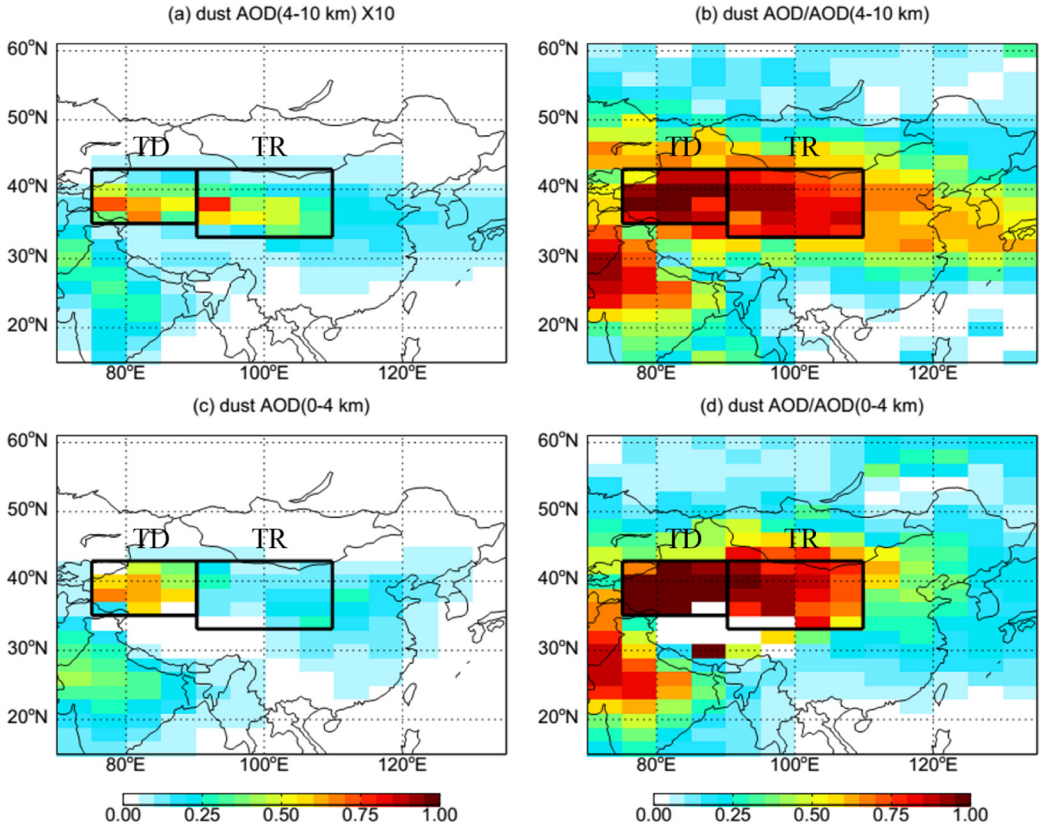

Fig. 7. Two layers of multiyear-mean dust AOD (left column) and the ratio of dust AOD (right column) to AOD over East Asia during spring of 2007–2016: the upper layer (4–10 km; upper row) and the lower layer (0–4 km; lower row). For a better display, dust AOD at the upper layer (4–10 km) is multiplied by 10. The black rectangles show the study region of TD and the transport region (TR, 90°–110° E, 33°–43° N).

Table 3
Definitions of High_4–6 km and Low_4–6 km using dust extinction at 4–6 km over TD during spring of 2007–2016 and Regional-mean statistics for vertical dust AOD differences over TD and the transported region (TR; 90°–110° E, 33°–43° N) of under these two conditions.

Conditions		High_4–6 km	Low_4–6 km	
Definitions		Dust extinction at 4–6 km ≥ the 80th percentile of the whole monthly mean over TD	Dust extinction at 4–6 km ≤ the 20th percentile of the whole monthly mean over TD	Difference between High_4–6 km and Low_4–6 km (%)
Dust AOD	At 1–4 km over TD	0.458	0.341	+34.3
	At 4–6 km over TD	0.066	0.016	+308.8
	At 4–10 km over TR	0.042	0.034	+23.7
	At 0–4 km over TR	0.159	0.226	−29.5
Dust AOD (4–10 km) in TR	90°–95°E	0.064	0.034	+89.2
	95°–100°E	0.039	0.034	+14.9
	100°–105°E	0.041	0.034	+18.7
	105°–110°E	0.023	0.033	−29.7

4, using the same method described above. Compared to Low_1–4 km, dust AOD over TD increase 158.2% at 1–4 km and 51.4% at 4–6 km respectively under the High_1–4 km condition (Table 4). However, there is no west-to-east gradient for dust AOD differences at 4–10 km over TR (Fig. 9) with even decreasing 10% and 7.6% over 90°–95°E and 95°–100°E (Table 4). Thus, high levels of dust under 4 km over TD are not the sufficient conditions for dust transport at 4–10 km over TR. When the increasing ratio of dust AOD at 4–6 km (+308.8%) is greatly more than that at 1–4 km (+34.3%) shown in Table 3, Taklimakan dust aerosols are more likely uplifted at high altitudes and entrained into dust transport outside of TD. It suggests that if there are more frequently weak dust events uplifting more dust aerosols below 4 km but not enough dust above 4 km, dust aerosols will be deposited locally and not transported outside of TD, leading to no gradient at 4–10 km over TR. When the increasing ratio of dust AOD at 4–6 km (+51.4%) is much less than that at 1–4 km (+158.2%) shown in Table 4, Taklimakan dust aerosols are more likely deposited locally due to the unique topography of TD. Consequently, the de-coupled interannual variability in this study is resulting from the two dust transport systems in TD.

To summarize, Taklimakan dust aerosols are more related to dust transport at high altitudes (4–10 km) than low altitudes (0–4 km) over downwind regions. High dust extinction below 4 km over TD is necessary but not sufficient conditions to ensure dust transport easterly, while high dust extinction levels at 4–6 km over TD are both necessary and sufficient conditions; such contrast leads to the de-coupled interannual variability seen by CALIOP.

5. Conclusions

In this study, we have investigated the interannual variation of dust vertical distribution over TD using monthly-mean CALIOP Level 3 products during MAM of 2007–2016. Taking dust extinction profiles and accepted dust sample profiles into account, we focus on dust extinction between 1 km and 6 km under the all-sky conditions. CALIOP 532 nm

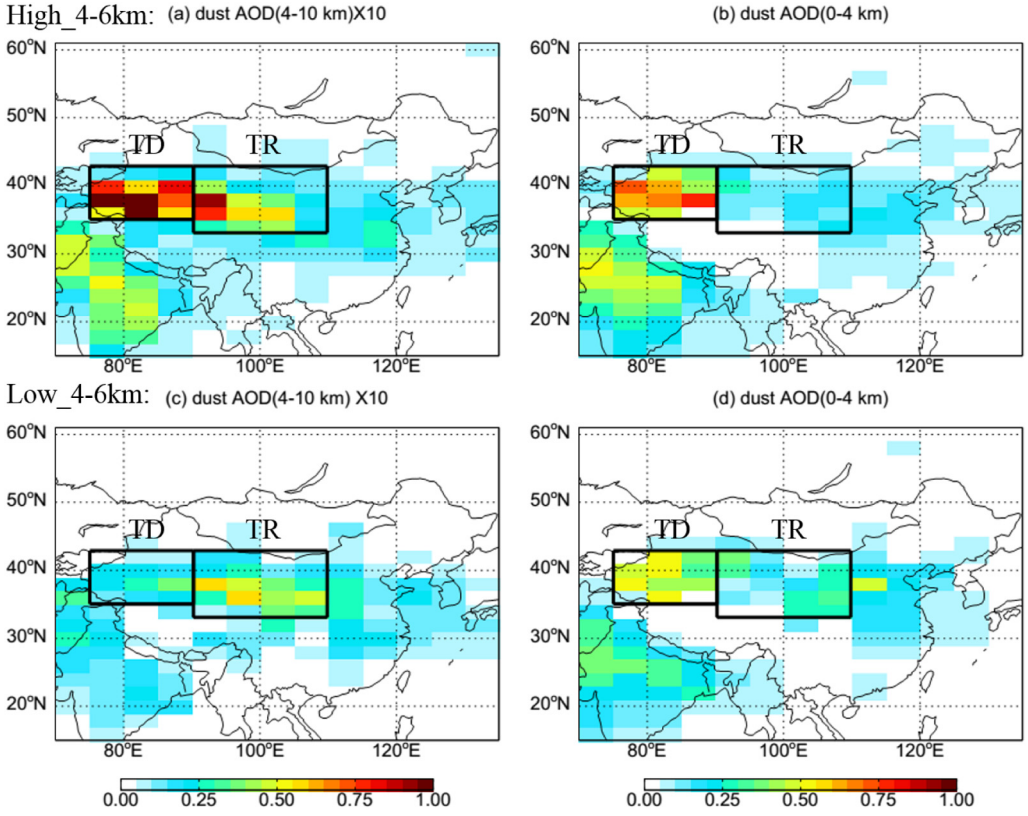

Fig. 8. Spatial distributions of dust AOD at 4–10 km (left column) and 0–4 km (right column) over East Asia under the 'High_4–6 km' condition (upper row) and the 'Low_4–6 km' condition (lower row) during spring of 2007–2016. For a better display, dust AOD at the upper layer (4–10 km) are multiplied by 10. 'High_4–6 km' and 'Low_4–6 km' are defined in Table 3. The black rectangles show the study region of TD and TR.

Table 4
Same as Table 3 but for 1–4 km over TD.

Conditions		High_1–4 km	Low_1–4 km	
Definitions		Dust extinction at 1–4 km ≥ the 80th percentile of the whole monthly mean over TD	Dust extinction at 1–4 km ≤ the 20th percentile of the whole monthly mean over TD	Difference between High_1–4 km and Low_1–4 km (%)
Dust AOD	At 1–4 km over TD	0.628	0.243	+158.2
	At 4–6 km over TD	0.041	0.027	+51.4
	At 4–10 km over TR	0.022	0.015	+42.3
	At 0–4 km over TR	0.377	0.336	+11.9
Dust AOD (4–10 km) in TR	90°–95°E	0.038	0.043	−10.0
	95°–100°E	0.032	0.034	−7.6
	100°–105°E	0.043	0.034	+24.7
	105°–110°E	0.038	0.023	+62.0

AOD generally agrees well with MODIS Deep Blue 550 nm AOD with correlation coefficient 0.62 for monthly-mean.

Dust extinction at each 1 km interval (1–2 km, 2–3 km, 3–4 km, 4–5 km and 5–6 km) has its distinct interannual variation. Dust extinction at 1–2 km, 2–3 km and 3–4 km show very similar interannual variations with each other and dust AOD, but the variations at 4–5 km and 5–6 km are very different from those below 4 km and dust AOD. Interannual variation of seasonal and monthly dust extinction at 1–4 km is almost as same as dust AOD ($R > 0.99$) and different from that at 4–6 km (R are around 0.42). There seems a distinct boundary at 4 km, consistent with the topography threshold of mineral dust from TD for long-range transport (Eguchi et al., 2009; Ge et al., 2014; Sun et al., 2001; Uno et al., 2009). We apply the comparison for four seasons of 2007–2016 and find that the de-coupled variability of dust extinction across 4 km over TD exists only in spring.

The Taklimakan Desert is a permanent arid desert, in which dust can be entrained to high altitudes by winds. Geographically, TD is surrounded by high mountains (average > 5 km) to the north, west and south. The prevailing wind directions in TD are easterly and northeasterly almost all year long (Ge et al., 2014; Sun et al., 2001). Thus, dust at elevations below 4 km cannot be easily transported out of this dessert (Huang et al., 2014; Sun et al., 2001). Our analysis provides observational evidence from CALIOP that vertical dust extinction over TD has distinctively different variability below and above 4 km altitude and this threshold divides dust transport in TD into two systems. Taklimakan dust aerosols are more related to dust transport at high altitudes (4–10 km) than low altitudes (0–4 km) over downwind regions. High dust extinction below 4 km over TD is necessary but not sufficient conditions to ensure dust transport easterly, while high dust extinction levels at 4–6 km over TD are both necessary and sufficient conditions; such contrast leads to the de-coupled interannual variability seen by CALIOP. The de-coupling of dust extinction profiles over TD may require verification with longer-term observations when more data become available in the future. The interannual variation of dust extinction between 1–4 km and 4–6 km identified here provides a useful metric that may be used to forecast dust concentrations and evaluate model performance in simulating long-term dust profile variability in China.

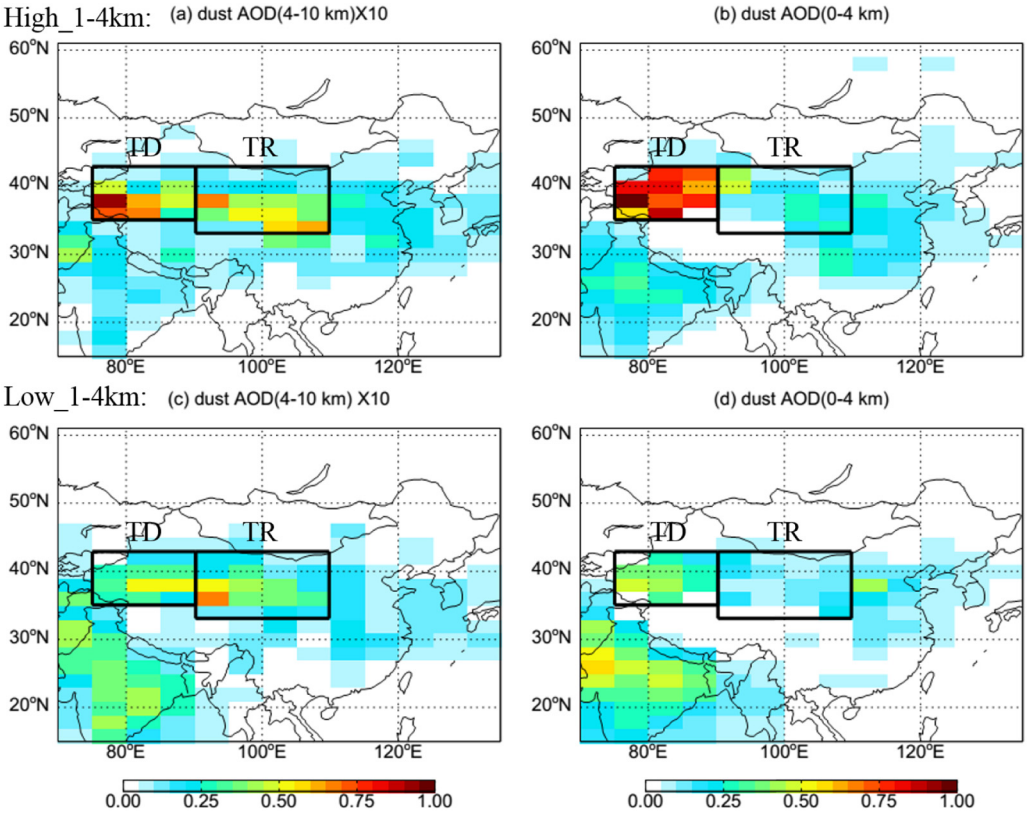

Fig. 9. Same as Fig. 8 but for 1–4 km over TD. 'High_1–4 km' and 'Low_1–4 km' are defined in Table 4.

Acknowledgment

This study was supported by the National Key Basic Research Program of China (2014CB441302 and 2013CB956603).

Appendix A. Supplementary data

Supplementary data to this article can be found online at https://doi.org/10.1016/j.scitotenv.2018.03.125.

References

Chen, S., Zhao, C., Qian, Y., Leung, L.R., Huang, J., Huang, Z., et al., 2014. Regional modeling of dust mass balance and radiative forcing over East Asia using WRF-Chem. Aeolian Res. 15, 15–30.

Chen, S., Huang, J., Li, J., Jia, R., Jiang, N., Kang, L., et al., 2017. Comparison of dust emissions, transport, and deposition between the Taklimakan Desert and Gobi Desert from 2007 to 2011. Sci. China Earth Sci. 1–18.

Eguchi, K., Uno, I., Yumimoto, K., Takemura, T., Shimizu, A., Sugimoto, N., et al., 2009. Trans-pacific dust transport: integrated analysis of NASA/CALIPSO and a global aerosol transport model. Atmos. Chem. Phys. 9, 3137–3145.

Ge, J., Huang, J., Xu, C., Qi, Y., Liu, H., 2014. Characteristics of Taklimakan dust emission and distribution: a satellite and reanalysis field perspective. J. Geophys. Res. Atmos. 119.

Ginoux, P., Prospero, J.M., Gill, T.E., Hsu, N.C., Zhao, M., 2012. Global-scale attribution of anthropogenic and natural dust sources and their emission rates based on MODIS deep blue aerosol products. Rev. Geophys. 50.

Grousset, F.E., Ginoux, P., Bory, A., Biscaye, P.E., 2003. Case study of a Chinese dust plume reaching the French Alps. Geophys. Res. Lett. 30 (10–1).

Hsu, N.C., Tsay, S.-C., King, M.D., Herman, J.R., 2006. Deep blue retrievals of Asian aerosol properties during ACE-Asia. IEEE Trans. Geosci. Remote Sens. 44, 3180–3195.

Huang, J., Minnis, P., Chen, B., Huang, Z., Liu, Z., Zhao, Q., et al., 2008. Long-range transport and vertical structure of Asian dust from CALIPSO and surface measurements during PACDEX. J. Geophys. Res. Atmos. 113.

Huang, J., Wang, T., Wang, W., Li, Z., Yan, H., 2014. Climate effects of dust aerosols over East Asian arid and semiarid regions. J. Geophys. Res. Atmos. 119.

Kim, M.H., Kim, S.W., Yoon, S.C., Omar, A.H., 2013. Comparison of aerosol optical depth between CALIOP and MODIS-Aqua for CALIOP aerosol subtypes over the ocean. J. Geophys. Res. Atmos. 118.

Liu, D., Wang, Z., Liu, Z., Winker, D., Trepte, C., 2008. A height resolved global view of dust aerosols from the first year CALIPSO lidar measurements. J. Geophys. Res. Atmos. 113.

Liu, Z., Vaughan, M., Winker, D., Kittaka, C., Getzewich, B., Kuehn, R., et al., 2009. The CALIPSO lidar cloud and aerosol discrimination: version 2 algorithm and initial assessment of performance. J. Atmos. Ocean. Technol. 26, 1198–1213.

Ma, X., Bartlett, K., Harmon, K., Yu, F., 2013. Comparison of AOD between CALIPSO and MODIS: significant differences over major dust and biomass burning regions. Atmos. Meas. Tech. 6, 2391–2401.

Omar, A.H., Winker, D.M., Vaughan, M.A., Hu, Y., Trepte, C.R., Ferrare, R.A., et al., 2009. The CALIPSO automated aerosol classification and lidar ratio selection algorithm. J. Atmos. Ocean. Technol. 26, 1994–2014.

Redemann, J., Vaughan, M., Zhang, Q., Shinozuka, Y., Russell, P., Livingston, J., et al., 2012. The comparison of MODIS-Aqua (C5) and CALIOP (V2 & V3) aerosol optical depth. Atmos. Chem. Phys. 12, 3025–3043.

Sayer, A., Hsu, N., Bettenhausen, C., Jeong, M.J., 2013. Validation and uncertainty estimates for MODIS collection 6 "deep blue" aerosol data. J. Geophys. Res. Atmos. 118, 7864–7872.

Sun, J., Zhang, M., Liu, T., 2001. Spatial and temporal characteristics of dust storms in China and its surrounding regions, 1960–1999: relations to source area and climate. J. Geophys. Res. Atmos. 106, 10325–10333.

Tanaka, T.Y., Chiba, M., 2006. A numerical study of the contributions of dust source regions to the global dust budget. Glob. Planet. Chang. 52, 88–104.

Textor, C., Schulz, M., Guibert, S., Kinne, S., Balkanski, Y., Bauer, S., et al., 2006. Analysis and quantification of the diversities of aerosol life cycles within AeroCom. Atmos. Chem. Phys. 6, 1777–1813.

Uno, I., Yumimoto, K., Shimizu, A., Hara, Y., Sugimoto, N., Wang, Z., et al., 2008. 3D structure of Asian dust transport revealed by CALIPSO lidar and a 4DVAR dust model. Geophys. Res. Lett. 35.

Uno, I., Eguchi, K., Yumimoto, K., Takemura, T., Shimizu, A., Uematsu, M., et al., 2009. Asian dust transported one full circuit around the globe. Nat. Geosci. 2, 557–560.

Winker, D.M., Vaughan, M.A., Omar, A., Hu, Y., Powell, K.A., Liu, Z., et al., 2009. Overview of the CALIPSO mission and CALIOP data processing algorithms. J. Atmos. Ocean. Technol. 26, 2310–2323.

Winker, D., Pelon, J., Coakley Jr, J., Ackerman, S., Charlson, R., Colarco, P., et al., 2010. The CALIPSO mission: a global 3D view of aerosols and clouds. Bull. Am. Meteorol. Soc. 91, 1211–1229.

Yu, H., Chin, M., Winker, D.M., Omar, A.H., Liu, Z., Kittaka, C., et al., 2010. Global view of aerosol vertical distributions from CALIPSO lidar measurements and GOCART simulations: regional and seasonal variations. J. Geophys. Res. Atmos. 115.

Yu, H., Remer, L.A., Chin, M., Bian, H., Tan, Q., Yuan, T., et al., 2012. Aerosols from overseas rival domestic emissions over North America. Science 337, 566–569.

Yu, H., Chin, M., Yuan, T., Bian, H., Remer, L.A., Prospero, J.M., et al., 2015. The fertilizing role of African dust in the Amazon rainforest: a first multiyear assessment based on data from cloud-aerosol lidar and infrared pathfinder satellite observations. Geophys. Res. Lett. 42, 1984–1991.

Yumimoto, K., Eguchi, K., Uno, I., Takemura, T., Liu, Z., Shimizu, A., et al., 2009. An elevated large-scale dust veil from the Taklimakan Desert: intercontinental transport and three-dimensional structure as captured by CALIPSO and regional and global models. Atmos. Chem. Phys. 9, 8545–8558.